

Supplementary Materials for

Nanoscale magnetic imaging of ferritins in a single cell

Pengfei Wang, Sanyou Chen, Maosen Guo, Shijie Peng, Mengqi Wang, Ming Chen, Wenchao Ma, Rui Zhang, Jihu Su, Xing Rong, Fazhan Shi, Tao Xu*, Jiangfeng Du*

*Corresponding author. Email: djf@ustc.edu.cn (J.D.); xutao@ibp.ac.cn (T.X.)

Published 10 April 2019, *Sci. Adv.* **5**, eaau8038 (2019)
DOI: 10.1126/sciadv.aau8038

This PDF file includes:

Section S1. Principle of spin noise measurement based on the NV center

Section S2. Calculation of the spin noise intensity $\langle B_{\perp}^2 \rangle$ from the single- τ measurement

Section S3. Point spread function of a single ferritin

Fig. S1. Experimental setup.

Fig. S2. Images of the nanopillars on diamonds.

Fig. S3. The treatment of FAC significantly increased the ferritins in HepG2 cells.

Fig. S4. Electron spin resonance spectra of resin-embedded HepG2 cells.

Fig. S5. The AFM characterization of the surface of cell sample.

Fig. S6. Adjusting the distance between the NV center and the cell section.

Fig. S7. Calculated spin noise intensity as a function of the distance between NV center and ferritin.

Fig. S8. Simulation of noise intensity at different vertical distances between a single ferritin and NV center.

Fig. S9. Trace data of Fig. 4A.

Reference (29)

Supplementary Materials

Section S1. Principle of spin noise measurement based on the NV center

The dynamic of the Fe^{3+} spins generates fluctuating magnetic field acting on the NV center. Such field enhances the relaxation rate of the electron spin of the NV center. To be specific, the component perpendicular to the NV axis, namely, transversal fluctuating field, induces flips of the NV electron spin, thus accelerating the longitudinal relaxation and resulting in a shorter relaxation time T_1 . The relaxation rate can be calculated as (22, 29)

$$\frac{1}{T_1} = \frac{1}{T_1^{\text{int}}} + \gamma^2 \langle B_{\perp}^2 \rangle \int S(\omega) F(\omega) d\omega \quad (\text{S1})$$

where $1/T_1^{\text{int}}$ is the intrinsic relaxation rate mainly attributed to the spin-lattice interaction, $1/T_1$ is the total relaxation rate in the presence of the fluctuating field, γ is the gyromagnetic ratio of the NV center, ω is the frequency, $S(\omega)$ is the normalized noise spectrum of the fluctuating field, $\langle B_{\perp}^2 \rangle$ is the transversal spin noise intensity on the NV center, and $F(\omega)$ is the filter function related to the experimental pulse sequence (22)

The variance of the transverse fluctuating field can be obtained by summing over the contributions of all the Fe^{3+} electron spins of the ferritin, namely

$$\langle B_{\perp}^2 \rangle = \sum_i \langle B_{\perp,i}^2 \rangle = \sum_i (\langle B_{x,i}^2 \rangle + \langle B_{y,i}^2 \rangle) = \sum_i \frac{1}{4} \left(\frac{\mu_0 \gamma_e \hbar}{4\pi} \right)^2 \frac{2 + 3 \sin^2 \theta_i}{r_i^6} \quad (\text{S2})$$

where θ_i is the inclination angle of the i th Fe^{3+} -NV vector with respect to the NV [111] axis.

Section S2. Calculation of the spin noise intensity $\langle B_{\perp}^2 \rangle$ from the single- τ measurement

The single- τ measurement was used to maximally shorten the data acquisition time. Before the NV MI, the depolarization curve of NV center was measured when the cell cube approached a blank zone on the diamond surface where no ferritin was in the detection range. The depolarization curve was normalized by the counts at $\tau = 0$ and fitted by the exponential decay, namely

$$F(\tau) = b + a e^{-\tau/T_1^{\text{int}}} \quad (\text{S3})$$

In the single- τ measurement, T_1 was acquired by solving the equation (S3) with the parameters a and b which were determined beforehand. The spectral density and filter function used in this work have the form (22)

$$S(\omega) = \frac{2}{\pi} \frac{\nu}{1 + (\omega\nu)^2}$$
$$F(\omega) = \frac{1}{\pi} \frac{\Gamma}{\Gamma^2 + (\omega - \omega_{+1})^2} + \frac{1}{\pi} \frac{\Gamma}{\Gamma^2 + (\omega - \omega_{-1})^2} \quad (\text{S3})$$

where $\Gamma = 1/T_{2NV}^*$ is the dephasing rate of the NV center electron spin with T_{2NV}^* being the dephasing time, ω_{+1} and ω_{-1} are the transition frequency of the NV center. The parameters of the spin noise are acquired by the experimental measurement shown in Fig. 2c. In X band electron paramagnetic resonance spectroscopy, there is a strong peak with $g = 2.0$ and the transverse relaxation rate of the Fe^{3+} spins is fitted to be 1.467 GHz. The correlation time of the noise spectrum is then found to be $\nu = (2\pi \times 1.467)^{-1}$ ns. We suppose that the transverse relaxation rate of Fe^{3+} is a constant in the magnetic field ranging from geomagnetic field to 3,500 Gauss. Then the spin noise intensity is acquired by solve the equation (S1).

Section S3. Point spread function of a single ferritin

For simplicity, we assume that the ferritin core is an ideal sphere and contains about 4,000 electron spins of Fe^{3+} . Fig. S7 shows the calculated spin noise intensity of ferritin as a function of the vertical distance between the NV center and the center of the ferritin. According to the spin noise intensity $\langle B^2 \rangle \sim 0.02$ mT² in Fig. 4C, the shortest vertical distance between ferritin and the NV center is estimated to be around 9 nm.

The point spread function (PSF) of a single ferritin protein in the unit of spin noise intensity is shown in Fig. S8. The full width at half maximum (FWHM) of the PSF at XY plane is around 10 nm at a vertical distance of 8 to 10 nm between the NV center and the center of a ferritin. In the XZ plane, a fast decay of the signal intensity in z direction is observed. This indicates high resolution in all directions.

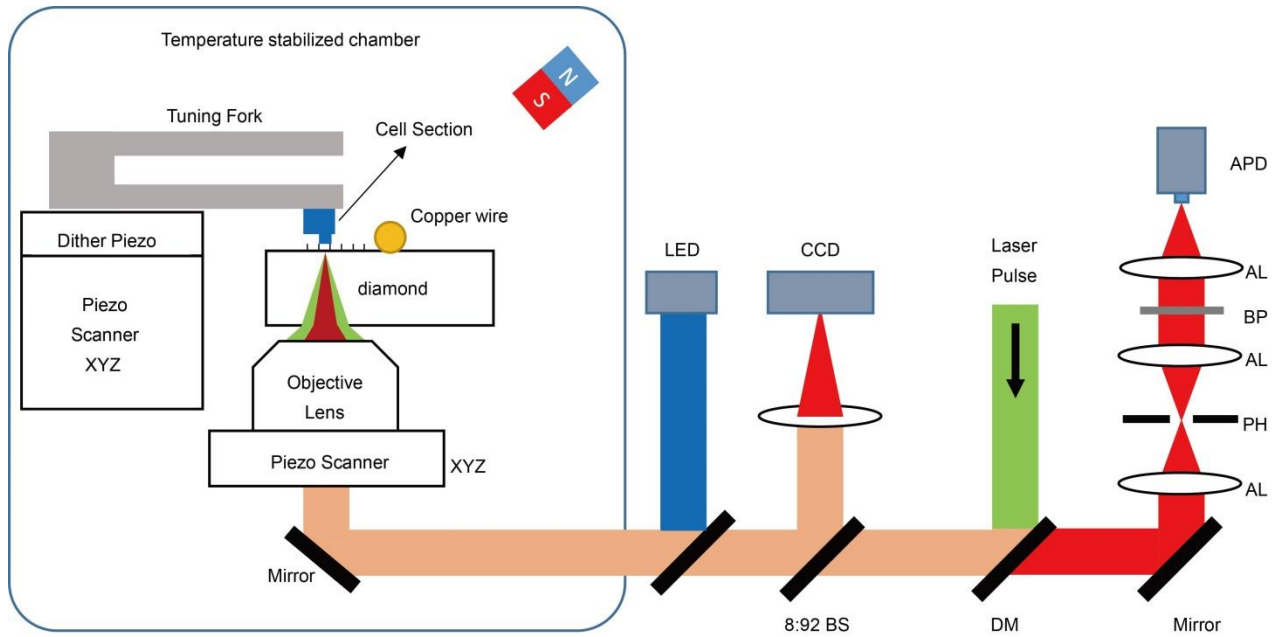


Fig. S1. Experimental setup. DM: dichroic mirror. BP: bandpass filter working at 650–775 nm. APD: avalanche photodiode. CCD: charge coupled device. LED: light emitting diode of 470 nm. AL: achromatic lens. PH: pinhole at a size of 30 μm . BS: beam splitter.

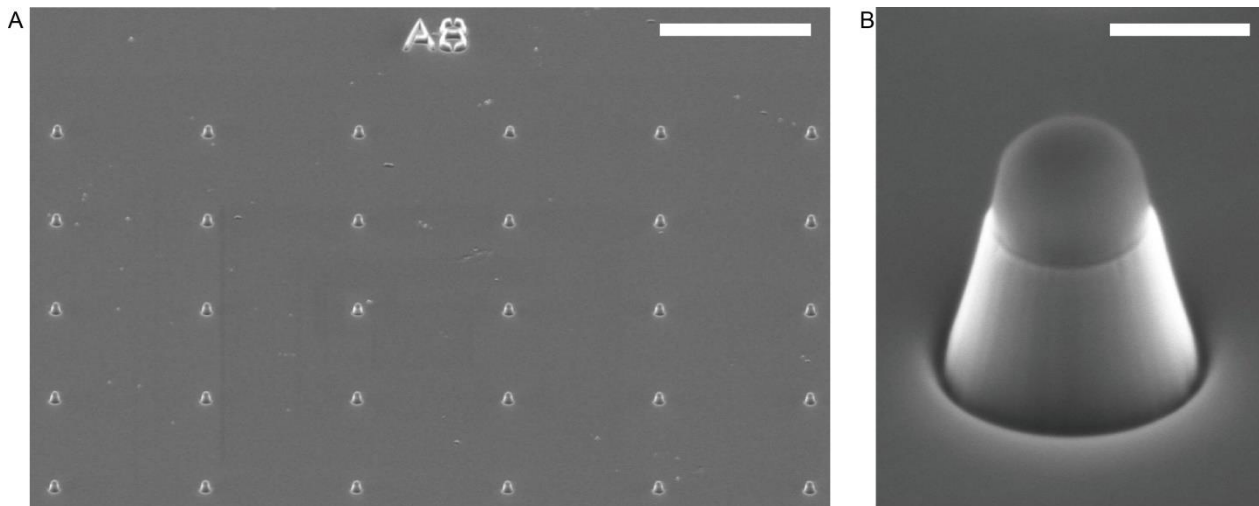


Fig. S2. Images of the nanopillars on diamonds. (A) SEM imaging of the fabricated diamond nanopillars just after reactive ion etching (RIE). The top of the nanopillar is covered by the HSQ to protect the NV center. (B) A single trapezoidal-cylinder shaped nanopillar. Scale bars, 10 μm (A); 400 nm (B).

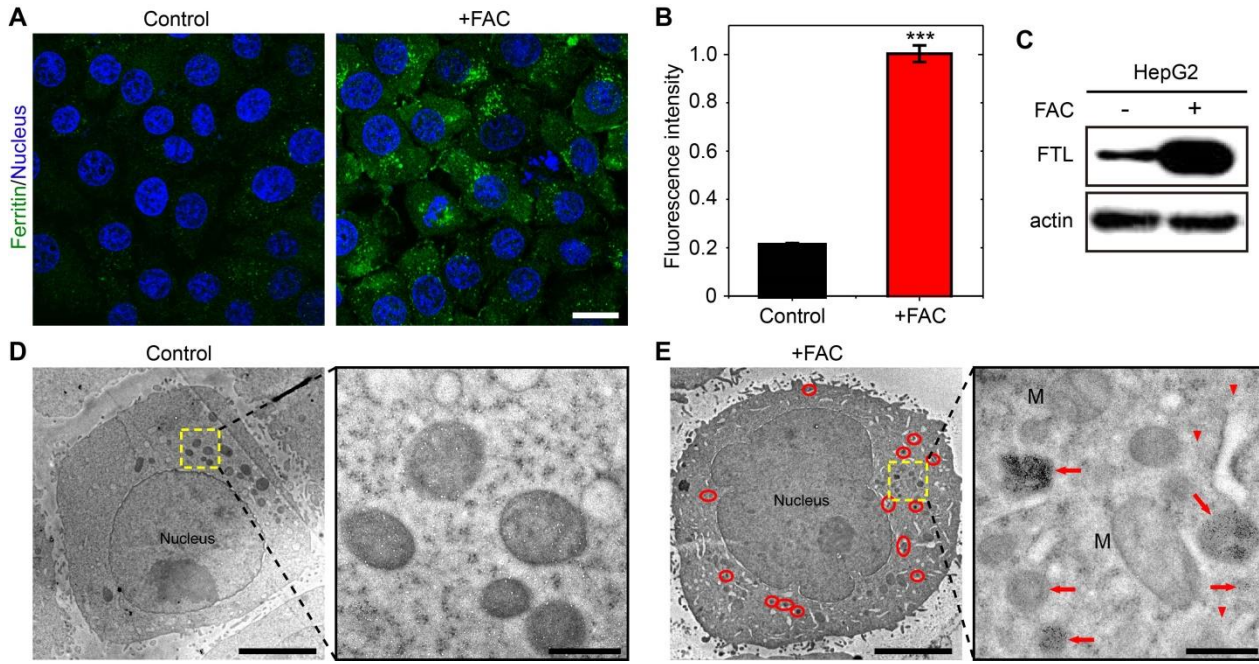


Fig. S3. The treatment of FAC significantly increased the ferritins in HepG2 cells. (A) The representative confocal images of control and FAC-stimulated HepG2 cells. The ferritin proteins were stained by anti-ferritin light chain (FTL) antibody in the green channel. The nuclei were indicated by DAPI in the blue channel. (B) The normalized average fluorescence intensity of HepG2 cells, as shown in (A) ($n = 53$ cells, control; $n = 88$ cells, FAC). $***P < 0.001$, Student's t test. Data are means \pm SEM. (C) The western blotting results of ferritin light chain in HepG2 cells with FAC-stimulation or no treatment. Actin was used as the loading control. (D and E) Transmission electron microscopy (TEM) images of control and FAC-treated HepG2 cells. Ferritin iron cores appear as spots of high electron density. We found that these spots specified as ferritins in FAC-treated cells were abundant, while they were absent in control cells. Red circles (whole cell) and arrows (zoomed image) in (E) indicate ferritin clusters. Few scattered ferritins are seen in the cytoplasm (arrowheads). M, mitochondrion. Scale bars, 20 μm (A); 5 μm (whole cells in D and E); 500 nm (zooms in D and E).

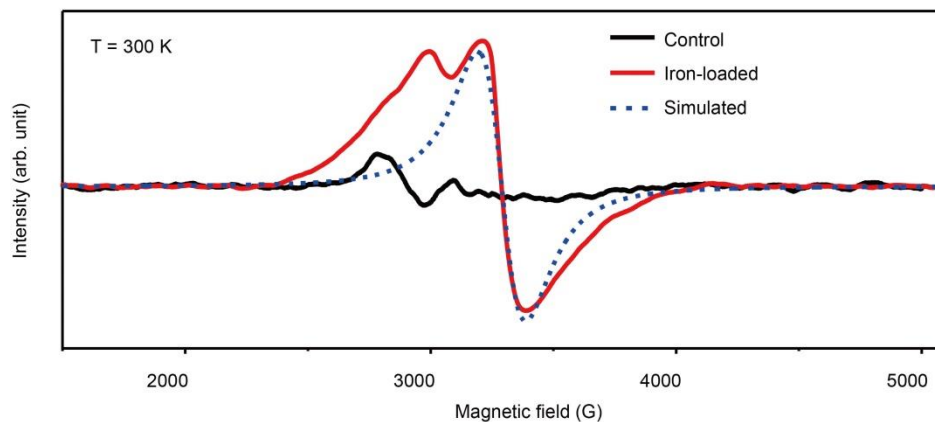


Fig. S4. Electron spin resonance spectra of resin-embedded HepG2 cells. The graph shows the normalized intensity of EPR spectra of control (black line) and Fe-loaded (red line) resin-embedded HepG2 cells at 300 K. The blue dash line indicates the simulated EPR spectrum of ferric iron.

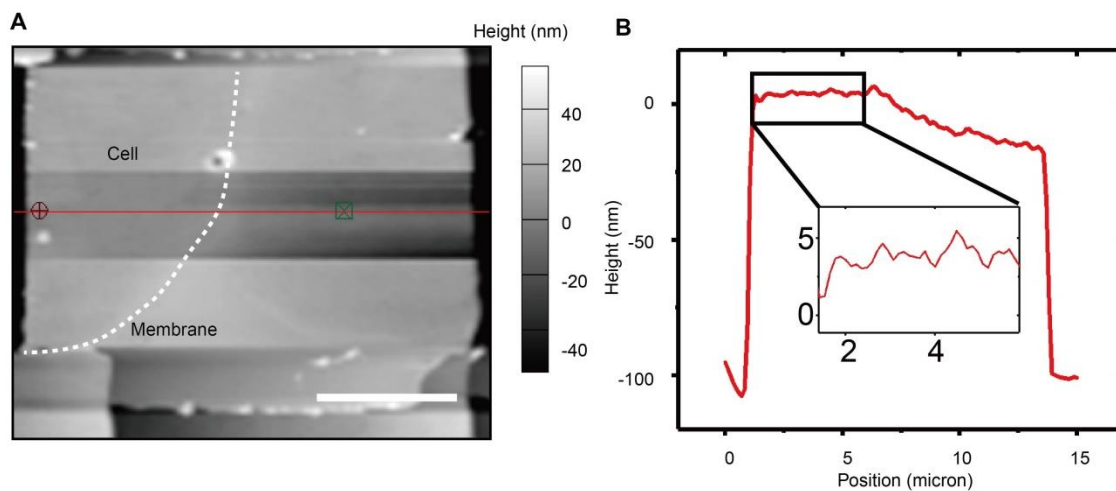


Fig. S5. The AFM characterization of the surface of cell sample. (A) AFM scanning of one of the cell cube. The figure is mask flattened by the Asylum Research AFM control software. The boundary between each cell is clear to view. The dark ribbon in the middle of the cell cube is because of Mask Flatten in AFM data analyzing process. (B) The trace data of the red line in (A). The enlarged inset figure shows the flatness of the cell region. Scale bar, 5 μm (A).

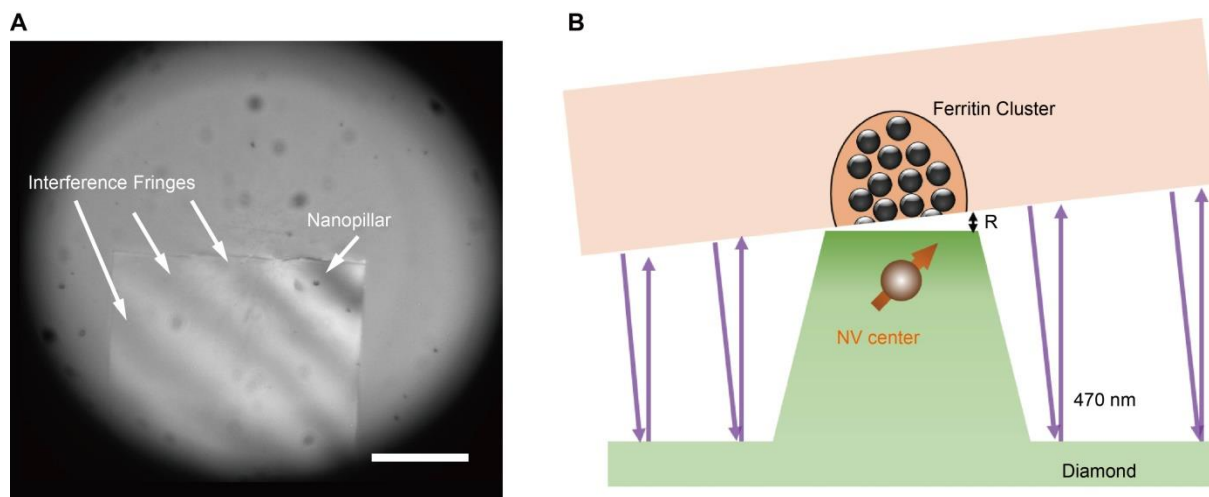


Fig. S6. Adjusting the distance between the NV center and the cell section. (A) Interference fringes between the cell cube and the diamond surface. Scale bar, 20 μm . (B) The geometric relation and the gap R between cell samples and diamond-pillars. The top surface diameter of the nanopillar is 400 nm.

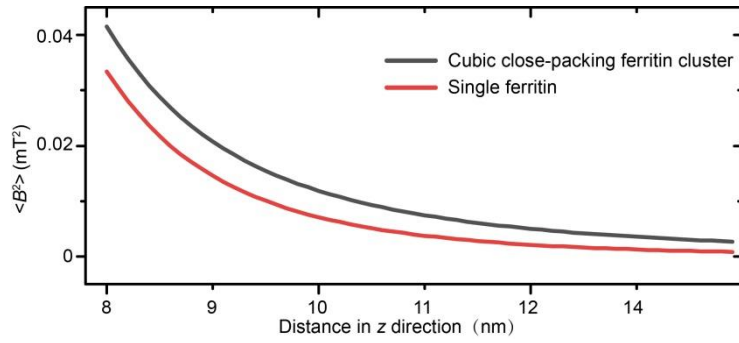


Fig. S7. Calculated spin noise intensity as a function of the distance between NV center and ferritin. We consider 4,000 Fe^{3+} in an 8 nm core, which is a typical situation after the FAC treatment to the cell. Both of the upper bond and lower bond are given. The upper bond is simulated by cubic close-packing model with a size of $(120 \text{ nm})^3$, and the lower bond is by a single ferritin.

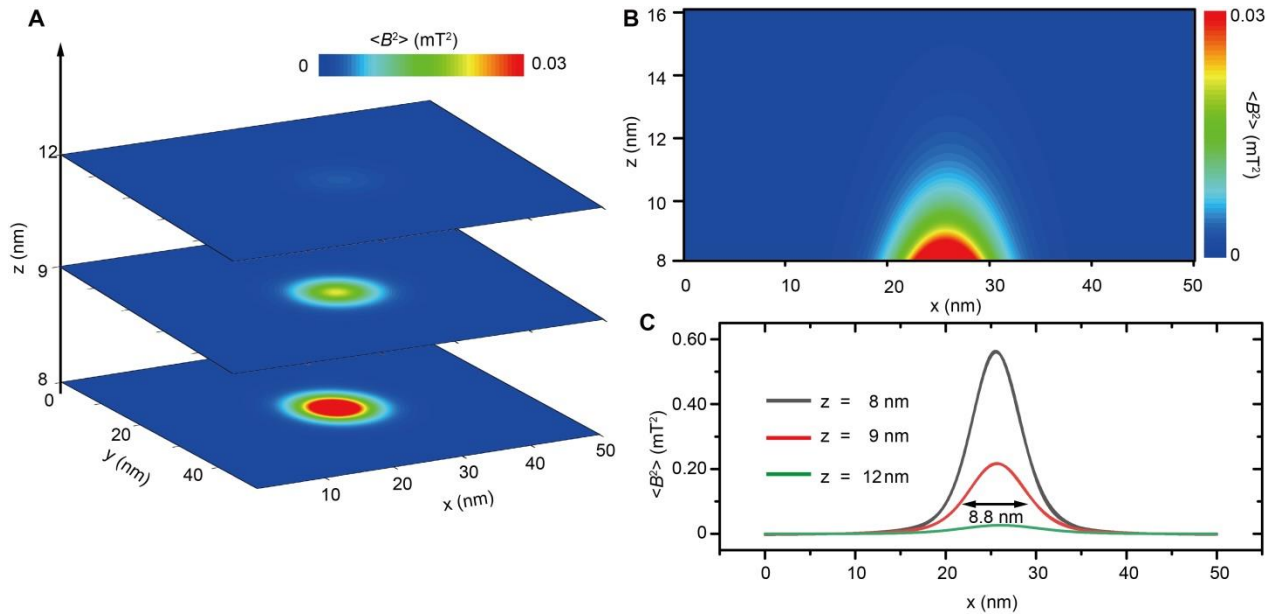


Fig. S8. Simulation of noise intensity at different vertical distances between a single ferritin and NV center. (A) XY 2D figure of normalized point spread function of a single ferritin molecule. (B) XZ 2D figure of the point spread function. (C) The trace data in A. The Voigt peak shape is used for fitting and the FWHM is acquired by $\text{FWHM} = 0.5346f_L + (0.2166f_L^2 + f_G^2)^{0.5}$. The resolution defined by FWHM is 7 nm, 8 nm, and 11 nm under $z = 8 \text{ nm}$, $z = 9 \text{ nm}$, and $z = 12 \text{ nm}$, respectively.

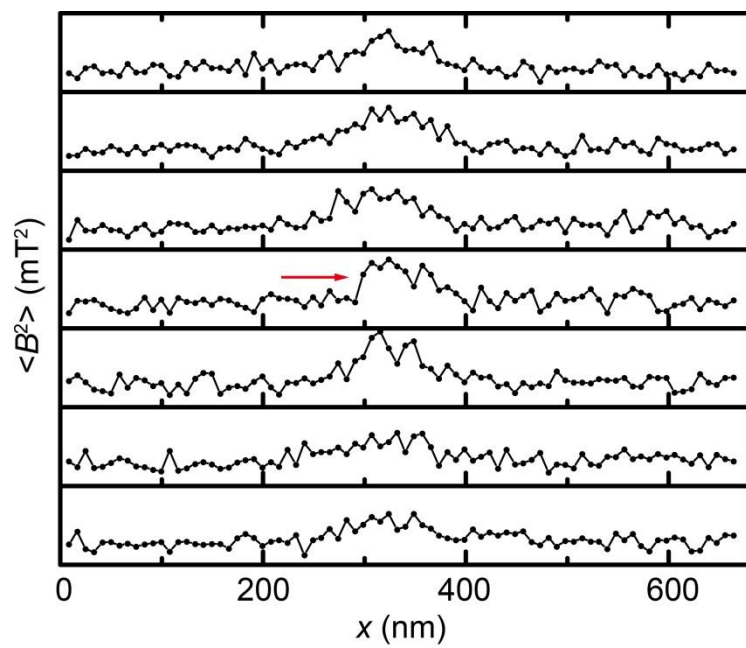


Fig. S9. Trace data of Fig. 4A. The red arrow points out the sharpest transition. The $\langle B^2 \rangle$ in every diagram is scaled from -0.01 mT^2 to 0.025 mT^2 .